

Circuit Design for Common-mode Noise Rejection in Biosignal Acquisition based on Imbalance Cancellation of Electrode Contact Resistance

Minghui Chen, Daisuke Anzai, Jianqing Wang,

Nagoya Institute of Technology, Department of Electrical & Mechanical Engineering

Nagoya, Japan

m.chen.032@stn.nitech.ac.jp, anzai@nitech.ac.jp,

wang@nitech.ac.jp

Georg Fischer

Friedrich-Alexander University of Erlangen-Nuremberg, Lehrstuhl für Technische Elektronik

Erlangen, Germany

georg.fischer@fau.de

Abstract—Common-mode (CM) noise is a primary interference to biological signal (biosignal) detection systems but is hardly solved with passive filtering. Conventionally, a driven-right-leg (DRL) circuit is employed to drive down the CM noise level. In this paper, we proposed a novel design of biosignal acquisition circuit based on canceling the imbalance between contact resistances of detection electrodes and made a comparison with the DRL circuit. We first theoretically analyzed how it works in rejecting the CM noise. Then we conducted circuit simulation and the result indicates that our design could realize a common-mode rejection of as high as 200 dB in experimental condition, which is better than the simulated DRL circuit.

Keywords—Common-mode noise, biosignal, biosignal detection, detection electrode, electromagnetic interference

I. INTRODUCTION

As the worldwide aging problem is drawing great attention, body area network (BAN) with wearable sensing technologies [1, 2] that collect vital data for health-state monitoring, is supposed to spread extensively in near future. Usually, the wearable biosignal sensors are attached to human body directly or not and a differential amplifier is used for detecting the change in voltage. There is always an imbalance of impedance at the attaching part, which allows the common-mode (CM) noise converting into a differential mode (DM) interference voltage [3,4]. The limitation in the Common-Mode Rejection Ratio (CMRR) of an amplifier is another reason. As a result, CM noise source like the power line, electromagnetic interference (EMI) or a wireless power transfer system can seriously interfere the detection progress. As a conventional solution, a driven-right-leg (DRL) circuit [5] can drive down the CM voltage by means of reducing the effective impedance of the acquisition circuit. In this study, we combine the idea of driving down the CM voltage and canceling the imbalance in contact resistance of detection electrodes [6] and provide a novel design of biosignal acquisition circuit. First, we theoretically show how our approach performs in reducing the CM noise. Then we conduct circuit simulations for comparing effect in reducing the interference of CM noise among a

conventional biosignal acquisition circuit, the DRL circuit and our design.

II. CIRCUIT ANALYSIS AND EVALUATION ON THE INFLUENCE OF IMBALANCE

At this part, we analyze three circuits and evaluate how much CM voltage will be produced when there is an imbalance in electrode contact resistance. Fig. 1 shows the CM equivalent circuit of a wearable ECG [4]. It has two detection electrodes and one ground electrode. The ECG signals are acquired from the two detection electrodes, and then differentially amplified with an operational amplifier (OP-AMP). The interference voltage V_{CM} is between the human body and the earth ground. The impedance of the two detection electrodes are denoted as Z_{ea} or Z_{eb} respectively. Usually they are imbalanced due to the different attachment conditions. In addition, the impedance between the human body and the ground is denoted as Z_{eg} .

In this CM equivalent circuit, V_{out1} divided by V_{CM} can be written as

$$\frac{V_{out1}}{V_{CM}} = \frac{j\omega C_s R_2 Z_{eg} (Z_{ea} - Z_{eb})}{\alpha + \beta + \gamma} \quad (1)$$

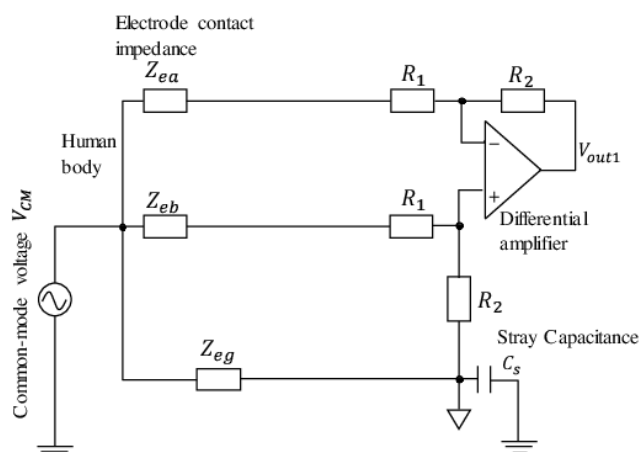


Fig. 1. The CM equivalent circuit of biosignal acquisition circuit in [4]

Where

$$\alpha = (Z_{ea} + Z_{eb} + 2R_1)Z_{eg} \quad (2)$$

$$\beta = (Z_{ea} + R_1)(Z_{eb} + R_1 + R_2) \quad (3)$$

$$\gamma = j\omega C_s(Z_{ea} + R_1)(Z_{eb} + R_1 + R_2)Z_{eg} \quad (4)$$

From (1) we can see that if the imbalance between the two detection electrodes is cancelled, the CM voltage V_{CM} could not be converted into DM output voltage. While, this fact happens to all the differential amplifying systems, as long as the stray capacitance C_s exists. The problem we would like to point out is that the system in Fig. 1 receives more influence from the imbalance between Z_{ea} and Z_{eb} than the other designs we are about to mention. The evaluation of this section is to show this problem quantitatively. The second circuit that we use for this comparison is a typical DRL Circuit shown in Fig. 2. The mechanism of the DRL Circuit is well known and Fig. 2 can be considered to be using the DRL technology in the same circumstances as Fig. 1 without considering about the filters. It should be noticed that the performance of the DRL circuit depends on the value of impedances at the feedback part (Z_R and Z_f). In our simulated circuit, Z_R is 10 K Ω and Z_f is 10 M Ω [5], as a usual combination for actual use. The third circuit we proposed for this comparison is the design shown in Fig. 3. In this circuit, we use two OP-AMPs as buffers to reduce the CM noise basing on the circuit in Fig. 1. The two OP-AMPs are considered to be non-ideal because if they are, the currents i_{b1} and i_{b2} become zero and the CM noise would not affect this circuit. On the other hand, the common mode input resistance of an OP-AMP could be as large as $10^9 \sim 10^{12} \Omega$, such that the currents i_{b1} and i_{b2} in Fig. 3 are approximately the same. Besides, the input offset voltage of the buffers are supposed to be very low such that the input and output voltages of them can be seen as equal. In this circuit, V_{out3} in Fig. 3 can be written as

$$\frac{V_{out3}}{V_{CM}} = \frac{j\omega C_s R_1 Z_{eg} (R_1 + R_2)(Z_{eg} + Z_{in})(Z_{ea} - Z_{eb})}{R_2(Z_{ea} + Z_{in})\Pi} \quad (5)$$

Where

$$\Pi = (1 + j\omega C_s Z_{eg})(R_1 + R_2)(Z_{eg} + Z_{in}) + Z_{eg}(Z_{ea} - Z_{eb} + Z_{in}) \quad (6)$$

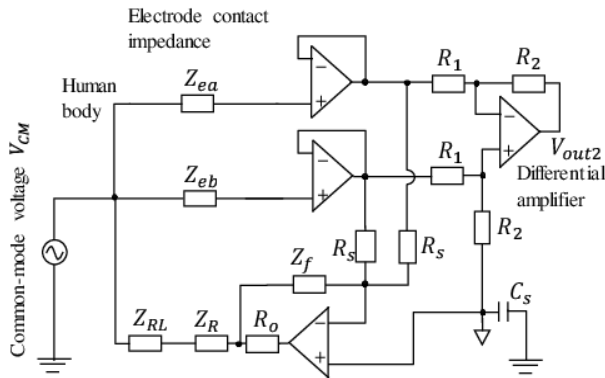


Fig. 2. The typical DRL circuit

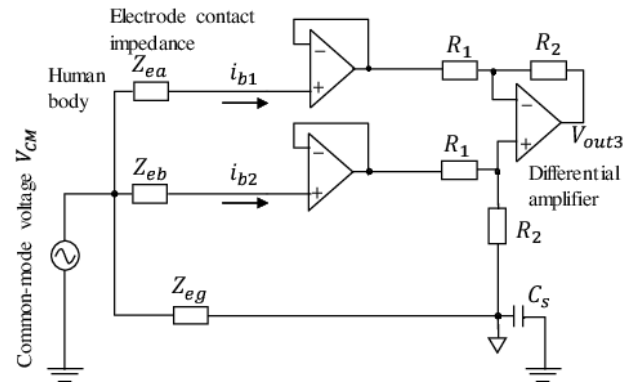


Fig. 3. The CM equivalent circuit of biosignal acquisition circuit with buffers

In order to understand (5) in a simple way, let $i_b = i_{b1} = i_{b2}$, then V_{out3} can be written as

$$V_{out3} = i_b \frac{R_2}{R_1} (Z_{ea} - Z_{eb}) \quad (7)$$

and it indicates that if we use proper OP-AMPs with high CM input resistance which could reduce i_b , then V_{out3} will be reduced as well (of course parameters like the offset voltage are also critical in actual circuit design). The simulation evaluation was conducted using SPICE (Simulation Program with Integrated Circuit Emphasis). Fig. 4 shows the conditions of our circuit simulation. It was an EOG acquisition circuit with three electrodes (two biopotential electrodes and one earth/Right-Leg electrode), coupled with the CM noise. An alternating current (AC) noise source at 60 Hz was assumed as the primary CM voltage source V_{CM} . It is coupled to the human body through C_1 . The three electrodes were attached to human body as in Fig. 1, 2 or 3. Capacitance C_s was coupled between earth ground and the signal ground. Primary imbalance between the Z_{ea} and Z_{eb} was assumed to be a difference in resistance. The parameters of the circuit components are shown in Table 1. The OP-AMPs used as buffers were all simulated with the model of OP-07 made by ANALOG DEVICE, which has high CM input resistance and very low offset voltage. The OP-AMPs for the DRL feedback and the differential amplifier were ideal because their influences were not our concern in this evaluation.

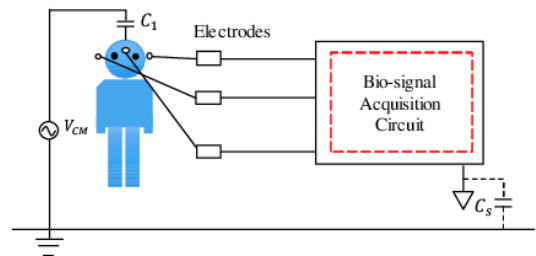


Fig. 4. Assumed simulation situations. The designs in Fig. 1, Fig. 2 and Fig. 3 are employed as the biosignal acquisition circuit respectively during the simulation.

TABLE I. PARAMETERS OF THE CIRCUIT COMPONENTS

Parameter	Value	Parameter	Value
Frequency	60 Hz	V_{CM}	20V Vpp
Z_{ea}	1 Ω ~200 K Ω	R_1	10 K Ω
Z_{eb}	100 K Ω	R_2	10 M Ω
Z_{eg}	10 K Ω	R_o	10 K Ω
Z_f	1 M Ω	R_s	10 K Ω
Z_{RL}	100 K Ω	C_s	200 pF
C_1	100 pF		

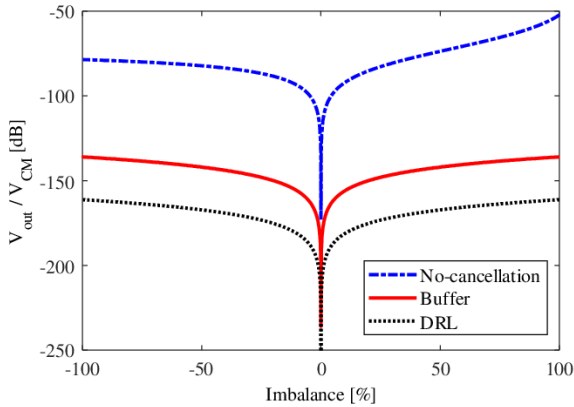


Fig. 5. Simulation results of the influence of imbalance in contact resistance. No-cancellation: result of the conventional circuit in Fig. 1. DRL: result of the DRL circuit in Fig. 2. Buffer: result of the circuit in Fig. 3.

The simulation result is shown in Fig. 5. The horizontal axis is the imbalance of contact resistances and the vertical axis is the ratio of V_{out} to V_{CM} in decibel (dB). The imbalance is calculated as

$$Imbalance = \frac{\delta R}{R} \times 100\% \quad (8)$$

For example, if the Z_{ea} is 110 K Ω and the Z_{eb} is 100 K Ω , then the imbalance is 10%. We can see that the V_{out}/V_{CM} is only -50 dB (or to say that the common-mode rejection is as low as 50 dB) when there is no proper cancelling measure. For an actual biosignal acquisition circuit, normally it can accomplish the task only if the V_{out}/V_{CM} is smaller than about -100 dB. This fact implies that the system in Fig. 1 can hardly work when there is an imbalance bigger than 2% between Z_{ea} and Z_{eb} . By comparing the three plots in Fig. 5, it is obvious that the DRL circuit exhibits the least interference and the addition of buffer is better than the one in Fig. 1. The reason is that the buffers in Fig. 2 and Fig. 3 reduces the CM currents flow through the acquisition circuit, and the negative feedback in DRL drives down the effective impedance of the whole acquisition circuit better than a single resistance Z_{eg} like in Fig. 3. In addition, the CM noise level becomes extremely low when the imbalance is near to zero.

III. IMBALANCE CANCELLATION DESIGN WITH DIGIPOTS AND EVALUATIONS

In Section 2 we showed to what extent an imbalance in the contact resistance can affect the three circuits. In this section, we show a design which uses digiPOTs to reduce the

imbalance in the contact resistance, such that the CM noise is reduced further. In [6], a design using CdS as a variable resistor, or a rheostat, to compensate the imbalance in contact resistance was proposed. In our design, we choose the digiPOTs as alternative because it not only can be well adjusted through a digital controlling circuit, but it also has bigger end-to-end resistance and better resolution of resistance. The models we have chosen are the TPL0102-100 and TPL0202-10 of Texas Instruments. Table 2 shows the main parameters of them.

TABLE II. THE PARAMETERS OF TPL0102-100 AND TPL0202-10

Parameter	TPL0102-100	TPL0102-10
Number of steps	256	256
Number of Channels	2	2
End-to-end resistance	100 K Ω	10 K Ω
Resolution	$\approx 390 \Omega$	$\approx 39 \Omega$

Fig. 6 shows the equivalent circuits of Fig. 1 and Fig. 3 with the digiPOTs installed.

For each channel, the end-to-end resistance of the TPL0102-100 is 100 K Ω with 256 taps and its resolution is about 390.6 Ω . Thus, if we use this digiPOT to reduce the imbalance, it can be adjusted to no more than about 390.6 Ω , in the range of 0 ~ 100 K Ω . In the case of the TPL0202-10, the end-to-end resistance is 10 K Ω . It also has two channels and 256 taps with a resolution of about 39.1 Ω . As a result, the range that it could function becomes smaller (0 ~ 10 K Ω), but it can make the imbalance be compensated to no more than 39.1 Ω . With the circuits shown in Fig. 6 simulated in SPICE, we can evaluate how well does the digiPOTs work in reducing the CM noise by cancelling the imbalance in resistance. Fig. 7 is the result of a comparison among the circuits in Fig. 1, Fig. 2 and Fig. 6(a). The parameters are mostly the same as shown in Table 1. The

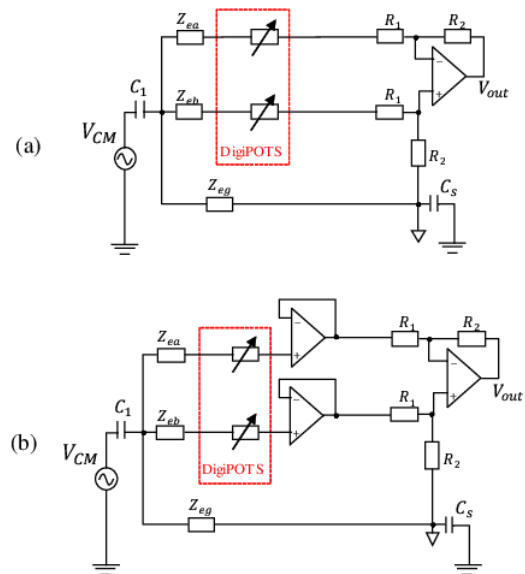


Fig. 6. CM equivalent circuit with the digiPOTs. (a) The circuit in Fig. 1 with digiPOTs installed. (b) The circuit in Fig. 3 with digiPOTs installed.

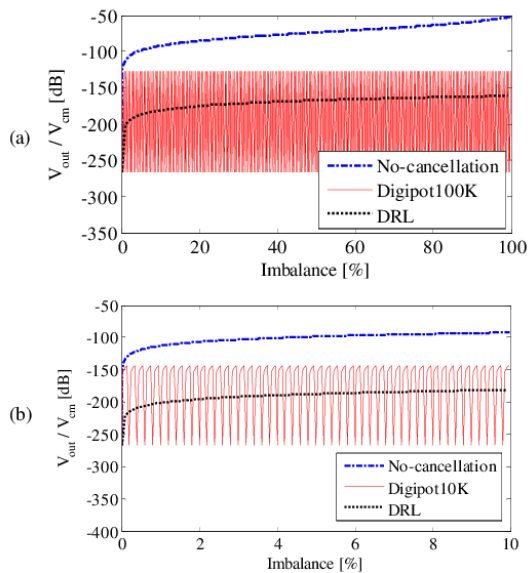


Fig. 7. Comparison of CM noise rejection performances among three circuits. “No-cancellation” and “DRL”: the same result as in Fig. 5. “DigiPOT100K” in (a): TPL0102-100 used in the circuit of Fig. 6 (a). “DigiPOT10K” in (b): TPL0202-10 used in the circuit of Fig. 6 (a).

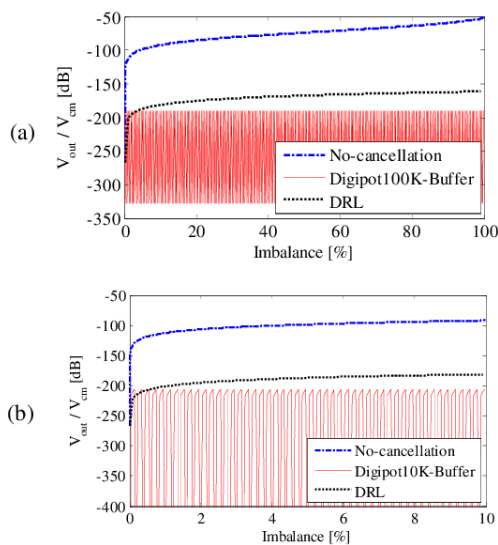


Fig. 8. Comparison of CM noise rejection performances among three circuits. “No-cancellation” and “DRL”: the same result as in Fig. 5. “DigiPOT100K-Buffer”: TPL0102-100 used in the circuit of Fig. 6 (b). “DigiPOT10K-Buffer”: TPL0202-10 used in the circuit of Fig. 6 (b).

results of using a TPL0102-100 or TPL0202-10 are shown respectively. The horizontal axis is the imbalance, whose calculation is given by (8). As is shown in Fig. 5, the influence of a positive imbalance (when Z_{eb} is bigger than Z_{ea}) or a negative imbalance (when Z_{ea} is bigger than Z_{eb}) do not have much difference, especially for the circuit in Fig. 2 and Fig. 3. Thus, we show the result at the range of from 0% to 100% for TPL0102-100, and 0% to 10% for TPL 0202-10 because its adjustable range is smaller. In Fig. 7, the imbalance is set to change by every 10 Ω , while the resistance of the digiPOT change by its resolution. As we used the TPL0102-100 in Fig. 7 (a), its resistance changed by every 390.6 Ω during the simulation. In Fig. 7 (b), the TPL0202-10 is used and its

resistance changed by every 39 Ω . Of course, the range of imbalance becomes 10 K Ω (the range of Imbalance becomes up to 10%). It should be noticed that in Fig. 7 (a) or (b), when the imbalance is compensated to almost the same as 0, the V_{out}/V_{CM} becomes extremely low (about -270 dB). However, as we cannot insure that the resistance of actual electrodes changes by every 390.6 Ω or 39 Ω , this figure shows frequent fluctuations. The worst case is determined by the resolution of the digiPOT, that is why the “DigiPOT10K” in Fig. 7 (b) shows a better rejecting effect. The best case is also affected by the resolution, but we can see that it does not have too much difference in Fig. 7(a) and Fig. 7(b). Indeed, what we are seeking for is a design that can exceed the DRL, while the result in Fig. 7 shows that using digiPOTs in the circuit in Fig. 1 is not capable of realizing our goal. In most cases, the DRL seems to work better in reducing the influence of the CM noise in Fig. 7. As we know that our design shown in Fig. 3 has less CM interference than the circuit in Fig. 1, there is a possibility that the circuit in Fig. 6 (b) works better than the DRL and Fig. 6(a). To verify this idea, we conducted a circuit simulation like the last one for the circuit of Fig. 6 (b). Fig. 8 shows the result of this evaluation. From Fig. 8, it is obvious that our design generally works better than the DRL circuit in rejecting the CM noise. By comparing Fig. 8(a) and Fig. 8(b), we can also find that the resolution of the digiPOT plays an important role in the rejecting effect of CM noise. In comparison with Fig. 7, we can see that the CM noise becomes smaller, and our design could have a better performance than the DRL circuit, especially when there is a large imbalance in the resistance.

IV. CONCLUSION

The biosignal acquisition plays an important role in the healthcare applications, and its accuracy and precision could be affected by the CM noise or EMI. In order to give a better design of biosignal acquisition circuit, we proposed a new circuit design based on canceling the imbalance in contact resistance of detection electrodes. The result of simulation shows that our design can accomplish a high CM noise rejection of more than 180 dB or 200 dB, which is about 20 ~ 40 dB better than the average performance of DRL. In summary, the approach we presented provides a novel idea of CM noise rejection, and it is capable of leading to a new design of biosignal acquisition to make the circuit smaller and the accuracy higher.

- [1] IEEE Std 802.15.6-2012, “IEEE Standard for local and metropolitan area networks - Part 15.6: Wireless Body Area Networks,” IEEE, 2012.
- [2] J. Wang, Q. Wang, *Body Area Communications*, Wiley-IEEE, 2012.
- [3] W. Liao, J. Shi and J. Wang, “An approach to evaluate electromagnetic interference with wearable ECG at frequencies below 1 MHz”, *IEICE Trans. Commun.*, vol.E98-B, no.8, pp.1606-1613, Aug. 2015.
- [4] W. Liao, J. Shi, J. Wang, “Electromagnetic interference of wirelesspower transfer system on wearable electrocardiogram,” *IET Microwaves Antennas & Propagation*, vol. 11, no. 3, pp. 330-335, 2017.
- [5] B. B. Winter, J. G. Webster, “Driven-right-leg circuit design,” *IEEE Transactions on Biomedical Engineering*, vol. BME-30, no. 1, pp. 62-66, 1983.
- [6] M. Noro, D. Anzai, J. Wang, “Common-mode noise cancellation circuit for wearable ECG,” *Healthcare Technology Letters*, vol. 4, no. 2, pp.64-67, 2017.